An International Journal of Optimization and Control: Theories & Applications
ISSN: 2146-0957 eISSN: 2146-5703
Vol.x, No.x, pp.xx-xx (2026)
https://doi.org/10.36922/IJOCTA026290166

RESEARCH ARTICLE

Quasi-Mittag-Leffler synchronization of delayed fractional-order Cohen-Grossberg inertial neural networks with uncertain parameters

Pavithra Ganeshan, Dharani Shanmugavel* and Sivakumar Muthusamy

Department of Mathematics, School of Advanced Sciences, Vellore Institute of Technology, Vellore, Tamil Nadu, India
pavithra.g2023@vitstudent.ac.in, s.dharani@vit.ac.in, sdharanimails@gmail.com

ARTICLE INFO

Article history:
Received: July 16, 2026
Revised: August 27, 2026
Accepted: September 4, 2026
Published Online: November 18, 2026

Keywords:
Fractional order
Cohen-Grossberg inertial neural network
Quasi-Mittag-Leffler synchronization
Adaptive controller

AMS Classification 2010:
26A33; 92B25; 92B20; 93C10

ABSTRACT

In this work, the quasi-Mittag-Leffler (QML) synchronization problem of fractional-order Cohen–Grossberg inertial neural networks (FOCGINNs) in the presence of uncertain parameters and time-varying delays is investigated. Initially, two control strategies, namely, a state-feedback controller and an adaptive controller, are developed to achieve QML synchronization. By employing these control strategies, sufficient synchronization conditions are established using Lyapunov stability theory in connection with the fractional-order Halanay inequality and the Razumikhin approach. Moreover, explicit synchronization error bounds are derived using the Mittag–Leffler function. Finally, numerical simulations validate the theoretical results, demonstrating the effectiveness of both controllers and confirming the robustness of the proposed synchronization framework.

CC BY

1. Introduction

A neural network (NN) is an artificial intelligence model inspired by the human brain. It can solve many types of technological problems and promote technological breakthroughs. In recent decades, NNs have gained significant attention in the field of dynamical system research due to their diverse applications, including associative memory,[1] pattern recognition,[2] and image processing.[3] Since time delays are inherent in practical systems and can significantly impair system performance, they may also induce complex dynamical behaviors, including oscillations[4] and bifurcations,[5,6] thereby motivating further investigation of delayed NN systems. As a result, delayed NNs have been extensively studied, and numerous findings have been documented in the existing literature.[7–10] Most existing studies on NN dynamics and synchronization have been limited to integer-order NNs. In contrast, the superior modeling capabilities of fractional calculus, characterised by its infinite memory and hereditary properties, are driving the development of fractional-order neural networks (FONNs). Recent research has highlighted the application of fractional calculus in NNs for stability, synchronization, optimization, and parameter training,[11] demonstrating its growing importance in the modeling and analysis of complex neural dynamics. The Cohen–Grossberg neural network (CGNN) model was originally introduced in 1983.[12] This general framework encompasses several well-known NN models, including bidirectional associative memory (BAM), Hopfield, and cellular NNs. The dynamical behavior of this model has attracted considerable attention in the literature.[13–15] In particular, numerous studies have investigated its stability,[16,17] stabilization,[18,19] and synchronization properties.[20,21]

Synchronization is a dynamical phenomenon in which systems with distinct initial conditions

*Corresponding Author

gradually achieve a desired relationship through mutual interactions or external control inputs. Extensive research has been devoted to synchronization in NNs,[20–22] motivated by its potential applications in areas such as cryptography, image processing, and secure information transmission. Recently, synchronization of fractional-order (FO) systems has attracted research interest and has progressed into an active research area, with various synchronization types such as finite-time,[23] projective,[24] quasi,[25] and complete synchronization. The synchronization analysis of delayed fractional-order Cohen–Grossberg neural networks (FOCGNNs) remains to be explored, which is one of the reasons behind this study. Notably, synchronization of delayed FOCGNNs has received considerable research attention and remains an active research topic.[26–28] Moreover, parameter uncertainties may arise in practical systems due to modeling inaccuracies and external perturbations, potentially affecting their dynamical behavior. Therefore, analyzing synchronization of NNs subject to time-varying delay (TVD) and parameter uncertainties is essential for ensuring reliable synchronization performance.

Compared with linear controllers,[29] nonlinear controllers,[30] and impulsive controllers,[31] adaptive controllers can reduce control costs while ensuring stable performance. Therefore, to achieve synchronization in NNs under uncertainties, the design of effective adaptive control schemes is important. Most research focuses on NNs defined solely by the first-order derivatives of state variables, neglecting the impact of inertial effects on system dynamics. To address this limitation, we focus on NNs that incorporate inertial effects. The concept of inertial NNs was introduced by Babcock and Westervelt in 1986 with the integration of inductors into traditional neural circuit models.[32] They demonstrated that the presence of inertial terms can result in complex and unusual dynamical phenomena, such as chaos, oscillatory behaviour, and instability. It should be noted that the incorporation of inertial effects into neural systems has specific biological backgrounds. The incorporation of inertial terms into CGNNs has significantly enriched their dynamical behaviors, and as a result, this topic has attracted considerable research interest, with several studies reported in the literature.[33–35] **Table 1** presents a comparison between the current study and previous research.

Inspired by the previous discussions, the QML synchronization of delayed FOCGNNs with parameter uncertainties and inertial terms will be investigated, and the major contributions are as follows:

- A fractional-order Cohen-Grossberg inertial neural network (FOCGINN) system of Caputo type with uncertain parameters and TVDs is considered. Through an appropriate variable transformation, the FOCGINNs are equivalently converted into the standard FOCGNN framework.
- To achieve QML synchronization between the FOCGINNs, state-feedback and adaptive control mechanisms are employed. The state-feedback controller stabilizes the synchronization error system, while the adaptive controller dynamically adjusts the control gains to accommodate parameter uncertainties.
- By utilizing the FO Halanay inequality and the Razumikhin technique, sufficient synchronization criteria are established by the Lyapunov stability theory, and the synchronization error bounds are explicitly estimated.

The remainder of this paper is organized as follows: Section 2 covers the basic definitions and lemmas. The model formulations are presented in Section 3. Section 4 discusses the main results in two subsections, one with a state-feedback controller and another with an adaptive controller. Numerical results and concluding remarks are provided in Sections 5 and 6, respectively.

Table 1. Comparison of recent literature with the proposed work

Study	**Fractional-order**	**Cohen-grossberg**	**Delay**	**Inertial term**	**QML**	**Uncertain parameters**
[27]	✓	✓	✓	-	-	-
[34]	✓	✓	-	✓	-	-
[36]	✓	-	✓	-	-	-
[37]	✓	✓	✓	-	-	-
[38]	✓	✓	✓	✓	-	-
[39]	✓	-	-	-	✓	-
This study	✓	✓	✓	✓	✓	✓

2. Preliminaries

Definition 1. [40] *Consider the function* $\mathfrak{C}(t) \in \mathbb{C}([a,b] \to \mathbb{R})$*, and let its Caputo fractional derivative of order* ϕ *be described as*

$$ {}^{C}{}_{0}\mathcal{D}_{t}^{\phi}\mathfrak{C}(t) = \frac{1}{\Gamma(1-\phi)} \int_{0}^{t} \frac{\mathfrak{C}^{'}(q)}{(t-q)^{\phi}} dq. $$

For ease of notation, the Caputo fractional derivative operator ${}^{C}{}_{0}\mathcal{D}_{t}^{\phi}$ *is hereafter denoted by* ${}_{0}\mathcal{D}_{t}^{\phi}$.

Definition 2. [40] *The one-parameter Mittag-Leffler (ML) function is*

$$ \mathcal{E}_{\theta}(v) = \sum_{k=0}^{\infty} \frac{v^{k}}{\Gamma(\theta k+1)}, \quad \mu > 0, $$

and the of two-parameter ML function is

$$ \mathcal{E}_{\theta,\hat{\theta}}(v) = \sum_{k=0}^{\infty} \frac{v^{k}}{\Gamma(\theta k+\hat{\theta})}, \quad \theta > 0, \hat{\theta} > 0. $$

Lemma 1. [41] *Let* $\mathfrak{C}(t) \in \mathbb{C}([t_0, +\infty] \to \mathbb{R})$ *and* $\phi \in (0,1)$*. Then*

$$ {}_{0}\mathcal{D}_{t}^{\phi}\mathfrak{C}^{2}(t) \leq 2\mathfrak{C}(t){}_{0}\mathcal{D}_{t}^{\phi}\mathfrak{C}(t). $$

Lemma 2. [42] *Consider the function* $\mathfrak{C}(t) \in \mathbb{C}([t_0, +\infty] \to \mathbb{R})$ *and* $\forall \mathfrak{K}^{*} \in \mathbb{R}$*. Then the following inequality holds:*

$$ {}_{0}\mathcal{D}_{t}^{\phi}[\mathfrak{C}(t) - \mathfrak{K}^{*}]^{2} \leq 2[\mathfrak{C}(t) - \mathfrak{K}^{*}]{}_{0}\mathcal{D}_{t}^{\phi}\mathfrak{C}(t). $$

3. Model formulation

The uncertain delayed FOCGINN is defined as

$$ \begin{aligned} {}_{0}\mathcal{D}_{t}^{2\phi}\alpha_i(t) &= -S_i\, {}_{0}\mathcal{D}_{t}^{\phi}\alpha_i(t) - \mathfrak{A}_i(\alpha_i(t)) \\ &\Big[\mathfrak{g}_i(\alpha_i(t)) - \sum_{j=1}^{n}(\mathfrak{P}_{ij} + \Delta\mathfrak{P}_{ij})\mathfrak{f}_{1j}(\alpha_j(t)) \\ &- \sum_{j=1}^{n}(\mathfrak{Q}_{ij} + \Delta\mathfrak{Q}_{ij})\mathfrak{f}_{2j}(\alpha_j(t-\eta(t)) \\ &- \mathfrak{I}_i(t)\Big], \end{aligned} \tag{1} $$

where $i = 1, 2, \ldots, n$, $\alpha_i(t)$ refers to the i^{th} neuron state at time t, $\mathfrak{A}_i(\cdot)$ represents the amplification function, and $\mathfrak{g}_i(\cdot)$ refers to the behavior function. $\mathfrak{P}_{ij}$ and $\mathfrak{Q}_{ij}$ represent the connection weights between the states i and j. $f(\cdot)$ denotes the activation function. $\eta(t)$ and $\mathfrak{I}_i(t)$ represent the TVD and external input, respectively. $\Delta\mathfrak{P}_{ij}$ and $\Delta\mathfrak{Q}_{ij}$ denote the parameter uncertainties, which are bounded and described by

$$ |\Delta\mathfrak{P}_{ij}| \leq \Lambda_{ij} \quad \textit{and} \quad |\Delta\mathfrak{Q}_{ij}| \leq \Gamma_{ij} $$

where $\Lambda_{ij} > 0$ and $\Gamma_{ij} > 0$.

Consider FOCGINNs (1) as a drive system, and let its associated response system be defined as

$$ \begin{aligned} {}_{0}\mathcal{D}_{t}^{2\phi}\beta_i(t) &= -S_i\, {}_{0}\mathcal{D}_{t}^{\phi}\beta_i(t) \\ &- \mathfrak{A}_i(\beta_i(t))[\mathfrak{g}_i(\beta_i(t)) \\ &- \sum_{j=1}^{n}(\mathfrak{P}_{ij} + \Delta\mathfrak{P}_{ij})\mathfrak{f}_{1j}(\beta_j(t)) \\ &- \sum_{j=1}^{n}(\mathfrak{Q}_{ij} + \Delta\mathfrak{Q}_{ij})\mathfrak{f}_{2j}(\beta_j(t-\eta(t)) \\ &- \mathfrak{I}_i(t) + \mathfrak{U}_i(t)], \end{aligned} \tag{2} $$

where $\mathfrak{U}_i(t)$ denotes the controller and is designed later.

For systems (1) and (2), we use the following variable transformation:

$$ \begin{aligned} \mathfrak{R}_{\alpha i}(t) &= {}_{0}\mathcal{D}_{t}^{\phi}\alpha_i(t) + \alpha_i(t), \\ \mathfrak{R}_{\beta i}(t) &= {}_{0}\mathcal{D}_{t}^{\phi}\beta_i(t) + \beta_i(t). \end{aligned} $$

Then systems (1) and (2) are equivalent to

$$ \begin{cases} {}_{0}\mathcal{D}_{t}^{\phi}\alpha_i(t) = -\alpha_i(t) + \mathfrak{R}_{\alpha i}(t), \\ {}_{0}\mathcal{D}_{t}^{\phi}\mathfrak{R}_{\alpha i}(t) = -(\mathfrak{S}_i - 1)\mathfrak{R}_{\alpha i}(t) \\ -(1-\mathfrak{S}_i)\alpha_i(t) \\ -\mathfrak{A}_i(\alpha_i(t))\Big[\mathfrak{g}_i(\alpha_i(t)) \\ -\sum_{j=1}^{n}(\mathfrak{P}_{ij} + \Delta\mathfrak{P}_{ij})\mathfrak{f}_{1j}(\alpha_j(t)) \\ -\sum_{j=1}^{n}(\mathfrak{Q}_{ij} + \Delta\mathfrak{Q}_{ij})\times \\ \mathfrak{f}_{2j}(\alpha_j(t-\eta(t))) - \mathfrak{I}_i(t)\Big] \end{cases} \tag{3} $$

and

$$ \begin{cases} {}_{0}\mathcal{D}_{t}^{\phi}\beta_i(t) = -\beta_i(t) + \mathfrak{R}_{\beta i}(t), \\ {}_{0}\mathcal{D}_{t}^{\phi}\mathfrak{R}_{\beta i}(t) = -(\mathfrak{S}_i - 1)\mathfrak{R}_{\beta i}(t) \\ -(1-\mathfrak{S}_i)\beta_i(t) \\ -\mathfrak{A}_i(\beta_i(t))\Big[\mathfrak{g}_i(\beta_i(t)) \\ -\sum_{j=1}^{n}(\mathfrak{P}_{ij} + \Delta\mathfrak{P}_{ij})\mathfrak{f}_{1j}(\beta_j(t)) \\ -\sum_{j=1}^{n}(\mathfrak{Q}_{ij} + \Delta\mathfrak{Q}_{ij})\times \\ \mathfrak{f}_{2j}(\beta_j(t-\eta(t))) - \mathfrak{I}_i(t) + \mathfrak{U}_i(t)\Big]. \end{cases} \tag{4} $$

Consider the error states $\mathfrak{E}_i(t) = \beta_i(t) - \alpha_i(t)$ and $\mathfrak{E}_{\mathfrak{R}i}(t) = \mathfrak{R}_{\beta i}(t) - \mathfrak{R}_{\alpha i}(t)$. From systems (3) and (4), the error system is obtained as follows:

$$ \begin{cases} {}_{0}\mathcal{D}_{t}^{\phi}\mathfrak{E}_i(t) \\ = -\mathfrak{E}_i(t) + \mathfrak{E}_{\mathfrak{R}i}(t) \\ {}_{0}\mathcal{D}_{t}^{\phi}\mathfrak{E}_{\mathfrak{R}i}(t) \\ = -(\mathfrak{S}_i - 1)\mathfrak{E}_{\mathfrak{R}i}(t) - (1-\mathfrak{S}_i)\mathfrak{E}_i(t) \\ -\mathfrak{A}_i(\beta_i(t))\mathfrak{g}_i(\beta_i(t)) + \mathfrak{A}_i(\alpha_i(t))\mathfrak{g}_i(\alpha_i(t)) \\ +\mathfrak{A}_i(\beta_i(t))\sum_{j=1}^{n}(\mathfrak{P}_{ij} + \Delta\mathfrak{P}_{ij})\mathfrak{f}_{1j}(\beta_j(t)) \\ \quad -\mathfrak{A}_i(\alpha_i(t))\sum_{j=1}^{n}(\mathfrak{P}_{ij} + \Delta\mathfrak{P}_{ij})\mathfrak{f}_{1j}(\alpha_j(t)) \\ +\mathfrak{A}_i(\beta_i(t))\sum_{j=1}^{n}(\mathfrak{Q}_{ij} + \Delta\mathfrak{Q}_{ij}) \\ \mathfrak{f}_{2j}(\beta_j(t-\eta(t))) \end{cases} \tag{5} $$

$$\begin{cases} -\mathfrak{A}_i(\alpha_i(t))\sum_{j=1}^{n}(\mathfrak{Q}_{ij}+\Delta\mathfrak{Q}_{ij}) \\ \mathfrak{f}_{2j}(\alpha_j(t-\eta(t)) \\ +\mathfrak{A}_i(\beta_i(t))\mathfrak{I}_i(t)-\mathfrak{A}_i(\beta_i(t))\mathfrak{I}_i(t)+\mathfrak{U}_i(t). \end{cases}$$

For the subsequent analysis, we use the following hypotheses.

H1: For every $\wr, \hat{\wr} \in \mathbb{R}$, there exist $\mathfrak{X}_j > 0$ and $\mathfrak{Y}_j > 0$ such that

$$|f_{1j}(\wr) - f_{1j}(\hat{\wr})| \leq \mathfrak{X}_j|\wr - \hat{\wr}|,$$
$$|f_{2j}(\wr) - f_{2j}(\hat{\wr})| \leq \mathfrak{Y}_j|\wr - \hat{\wr}|.$$

H2: For every $\mathfrak{d} \in \mathbb{R}$, there exist constants $l_j^x > 0, l_j^\tau > 0$ and $\tilde{l}_j > 0$ satisfying the following:

$$|f_{1j}(\mathfrak{d})| \leq l_j^x, \quad |f_{2j}(\mathfrak{d})| \leq l_j^\tau, \quad |\mathfrak{I}_i(\mathfrak{d})| \leq \tilde{l}_i.$$

H3: Consider the function $\xi_i(\alpha_i) = \mathfrak{A}_i(\alpha_i)\mathfrak{g}_i(\alpha_i)$, which has a bounded derivative with respect to α_i and satisfies the following inequality:

$$0 \leq \underline{\xi}_i \leq \xi_i'(\alpha_i) \leq \bar{\xi}_i, \qquad i = 1, 2, \ldots, n,$$

where $\underline{\xi}_i > 0$ and $\bar{\xi}_i > 0$.

H4: Consider the function $\mathfrak{A}_i(\alpha_i(t))$ $(i = 1, 2, \ldots, n)$, which is bounded and has a bounded derivative and satisfies the following inequality:

$$0 \leq \underline{\mathfrak{A}}_i \leq \mathfrak{A}_i(\alpha_i(t)) \leq \bar{\mathfrak{A}}_i, \quad |\mathfrak{A}_i'(\cdot)| \leq \lambda_i,$$

where $\underline{\mathfrak{A}}_i > 0, \bar{\mathfrak{A}}_i > 0$ and $\lambda_i > 0$.

Remark 1. *The practical significance of the above hypotheses is explained as follows. H1 assumes Lipschitz continuity of the activation functions $f_{1j}(\cdot)$ and $f_{2j}(\cdot)$, which ensures that bounded variations in neuronal states produce proportionally bounded variations in the corresponding activation outputs. Such regularity is commonly adopted in NN stability and synchronization analysis. H2 imposes boundedness on the activation and interaction functions, ensuring that the nonlinear responses and inter-neuronal interactions remain within finite ranges, which is consistent with bounded operating ranges commonly considered in NN models. H3 requires the combined function $\xi_i(\alpha_i) = \mathfrak{A}_i(\alpha_i)\mathfrak{g}_i(\alpha_i)$ to be bounded and non-decreasing, which provides a controlled nonlinear response and facilitates the estimation of the Cohen–Grossberg terms in the synchronization analysis. H4 assumes that the amplification function $\mathfrak{A}_i(\alpha_i(t))$ is positive and bounded with a bounded derivative, ensuring that the amplification mechanism remains finite and varies at a controlled rate. These properties are practically meaningful for describing regular and bounded neuronal dynamics and are essential for establishing the stability and synchronization conditions of the considered system.*

Definition 3. [36] *System (1) is said to attain QML synchronization with system (2), with an error bound $\mathfrak{e}$ and the rate of convergence θ, if for all initial states satisfiying $\mathfrak{E}(s)$ $(s \in [\eta_{\max}, 0])$, there exist constants $\mathfrak{M} > 0, c > 0$, and $t_\eta > 0$ such that for $\forall t > t_\eta$, the error state satisfies*

$$\|\mathfrak{E}(t)\| \leq \{\mathfrak{M}\mathcal{E}_\phi(-\theta t^\phi)\}^c + \mathfrak{e}.$$

Remark 2. *When $\mathfrak{e} = 0$, the QML synchronization reduces to the ML synchronization. For $\phi = 1$ and $\mathfrak{e} = 0$, the system achieves exponential synchronization.*

Remark 3. *In,[36] the authors explored QML projective synchronization in delayed FONNs with mismatched parameters. In,[37] the authors studied the quasi-synchronization of FOCGNNs. In contrast to,[36,37] this work analyzes the QML synchronization of delayed FOCGNNs with uncertain parameters and inertial effects.*

Lemma 3. [43] *Consider a positive definite function $\mathfrak{C}(t)$ that satisfies the following*

$${}_0\mathcal{D}_t^\phi \mathfrak{C}(t) \leq -\Theta_1\mathfrak{C}(t) + \Theta_2 \max_{t-\eta(t)\leq s\leq t} \mathfrak{C}(s) + \Theta_3,$$
$$t > 0, \mathfrak{C}(s) = |\nu(s)|, \quad \eta_{\max} \leq s \leq 0,$$

where $\Theta_2 \geq 0, \Theta_3 \geq 0, \Theta_1 + \Theta_2 \leq 0$ and $\eta(t) \in [0, \eta_{\max}]$. Then there exists $\mathfrak{M}$ such that the following holds

$$\mathfrak{C}(t) \leq \mathfrak{M}\mathcal{E}_\phi(\kappa t^\phi) - \frac{\Theta_3}{\Theta_1 + \Theta_2}$$

for all $t \geq \eta(t) + 1$, where the parameter κ is defined as

$$\kappa = \sup_{t-\eta(t)\geq 1}\{\hat{\kappa}|\hat{\kappa} - \Theta_1 - \Theta_2\frac{\mathcal{E}_\phi(\hat{\kappa}(t-\eta(t))^\phi)}{\mathcal{E}_\phi(\hat{\kappa}t^\phi)} = 0\}.$$

Lemma 4. [44] *Consider non-negative functions $\mathfrak{C}(t)$ and $\hat{\mathfrak{C}}(t)$ that are continuous on $[0, +\infty]$, with $\mathfrak{C}(t)$ bounded on $[-\eta_{\max}, 0]$, satisfiying*

$${}_0\mathcal{D}_t^\phi(\mathfrak{C}(t) + \hat{\mathfrak{C}}(t)) \leq -\Theta_1\mathfrak{C}(t) + \Theta_2 \sup_{t-\eta(t)\leq s\leq t} \mathfrak{C}(s) + \Theta_3,$$

where $\phi \in (0, 1), \Theta_1 > \Theta_2 > 0$ and $\Theta_3 \geq 0$. For any $\mathcal{W} > 0$, there exists $T > 0$ such that

$$\mathfrak{C}(t) \leq \frac{\left(\mathfrak{C}(0) + \hat{\mathfrak{C}}(0) - \frac{\Theta_3}{\Theta_1}\right)\mathcal{E}_\phi(-\Theta_1 t^\phi) + \frac{\Theta_3}{\Theta_1}}{1 - \frac{\Theta_2}{\Theta_1}} + \mathcal{W},$$

$t > T$.

4. Main results

This section explores the FOCGINN's QML synchronization criteria through two different controller types: state-feedback controllers and adaptive controllers.

4.1. State-feedback controllers

The state-feedback control scheme is proposed as

$$\mathfrak{U}_i(t) = -\mathfrak{K}_{ai}\mathfrak{E}_i(t) - \mathfrak{K}_{bi}\mathfrak{E}_{\mathfrak{R}i}(t), \tag{6}$$

where $\mathfrak{K}_{ai} > 0$ and $\mathfrak{K}_{bi} > 0$ are control gains.

Theorem 1. *Under hypotheses (H2)–(H4), if the control parameters $\mathcal{K}_{ai}$ and $\mathcal{K}_{bi}$ satisfiying the following conditions*

$$\begin{cases} \mathfrak{I}_a = min(\mathfrak{I}_1, \mathfrak{I}_2) \geq 0, \\ \mathfrak{I}_b = \max_{1\leq i\leq n}\Big\{\bar{\mathfrak{A}}_i(|\mathfrak{Q}_{ij} + \Gamma_{ij}|)\mathfrak{Y}_j\Big\} \geq 0, \\ \mathfrak{I}_c = \sum_{i=1}^{n}\sum_{j=1}^{n}\Big[(\bar{\mathfrak{A}}_i(|\mathfrak{P}_{ij} + \Lambda_{ij}|)l_x)^2 \\ +(\bar{\mathfrak{A}}_i(|\mathfrak{Q}_{ij} + \Gamma_{ij}|)l_\tau)^2\Big] \geq 0, \end{cases} \tag{7}$$

where

$$\begin{aligned} \mathfrak{I}_1 = \min_{1\leq i\leq n}\Big\{&\underline{\xi}_i + 2 + \lambda_i\tilde{l}_i + |\mathfrak{S}_i| \\ &- \sum_{j=1}^{n}\bar{\mathfrak{A}}_i(|\mathfrak{P}_{ij} + \Lambda_{ij}|)\mathfrak{X}_j + \mathfrak{K}_{ai}\Big\}, \\ \mathfrak{I}_2 = \min_{1\leq i\leq n}\Big\{&\underline{\xi}_i + \lambda_i\tilde{l}_i + 3|\mathfrak{S}_i| - 4 - 4n + \mathfrak{K}_{ai} + 2\mathfrak{K}_{bi} \\ &- \sum_{j=1}^{n}\big[\bar{\mathfrak{A}}_i(|\mathfrak{P}_{ij} + \Lambda_{ij}|)\mathfrak{X}_j - \bar{\mathfrak{A}}_i(|\mathfrak{Q}_{ij} + \Gamma_{ij}|)\mathfrak{Y}_j\Big\}, \end{aligned}$$

then system (1) can achieve QML synchronization with system (2) under controller (6) with an error bound $\sqrt{\frac{\mathfrak{I}_c}{\mathfrak{I}_a - \mathfrak{I}_b}}$.

Proof Let us consider the Lyapunov function

$$\mathfrak{V}(t) = \sum_{i=1}^{n}\mathfrak{E}_i^2(t) + \sum_{i=1}^{n}\mathfrak{E}_{\mathfrak{R}i}^2(t). \tag{8}$$

Taking the fractional derivative of (8) based on Lemma 1 along (5), we have

$$\begin{aligned} {}_0\mathcal{D}_t^{\phi}\mathfrak{V}(t) &= 2\sum_{i=1}^{n}\mathfrak{E}_i(t){}_0\mathcal{D}_t^{\phi}\mathfrak{E}_i(t) \\ &+ 2\sum_{i=1}^{n}\mathfrak{E}_{\mathfrak{R}i}(t){}_0\mathcal{D}_t^{\phi}\mathfrak{E}_{\mathfrak{R}i}(t) \\ \leq& 2\sum_{i=1}^{n}\mathfrak{E}_i(t)\Big[\mathfrak{E}_{\mathfrak{R}i}(t) - \mathfrak{E}_i(t)\Big] \\ &+ 2\sum_{i=1}^{n}\mathfrak{E}_{\mathfrak{R}i}(t)\Big[-(\mathfrak{S}_i - 1)\mathfrak{E}_{\mathfrak{R}i}(t) \\ &- (1 - \mathfrak{S}_i)\mathfrak{E}_i(t) - \mathfrak{A}_i(\beta_i(t))\mathfrak{g}_i(\beta_i(t)) \\ &+ \mathfrak{A}_i(\alpha_i(t))\mathfrak{g}_i(\alpha_i(t)) \\ &+ \mathfrak{A}_i(\beta_i(t))\sum_{j=1}^{n}(\mathfrak{P}_{ij} + \Delta\mathfrak{P}_{ij})\mathfrak{f}_{1j}(\beta_j(t)) \\ &- \mathfrak{A}_i(\alpha_i(t))\sum_{j=1}^{n}(\mathfrak{P}_{ij} + \Delta\mathfrak{P}_{ij})\mathfrak{f}_{1j}(\alpha_j(t)) \\ &+ \mathfrak{A}_i(\beta_i(t))\sum_{j=1}^{n}(\mathfrak{Q}_{ij} + \Delta\mathfrak{Q}_{ij})\mathfrak{f}_{2j}(\beta_j(t - \eta(t)) \\ &- \mathfrak{A}_i(\alpha_i(t))\sum_{j=1}^{n}(\mathfrak{Q}_{ij} + \Delta\mathfrak{Q}_{ij})\mathfrak{f}_{2j}(\alpha_j(t - \eta(t)) \\ &+ \mathfrak{A}_i(\beta_i(t))\mathfrak{I}_i(t) - \mathfrak{A}_i(\beta_i(t))\mathfrak{I}_i(t) \\ &- \mathfrak{K}_{ai}\mathfrak{E}_i(t) - \mathfrak{K}_{bi}\mathfrak{E}_{\mathfrak{R}i}(t)\Big]. \end{aligned} \tag{9}$$

By H1 and H2, we obtain

$$\begin{aligned} &\mathfrak{A}_i(\beta_i(t))\mathfrak{g}_i(\beta_i(t)) - \mathfrak{A}_i(\alpha_i(t))\mathfrak{g}_i(\alpha_i(t)) \\ &\qquad = \xi_i^{'}(\chi_i(t))(\beta_i(t) - \alpha_i(t)), \\ &\mathfrak{A}_i(\beta_i(t)) - \mathfrak{A}_i(\alpha_i(t)) \\ &\qquad = \mathfrak{A}^{'}(\hat{\chi}_i(t))(\beta_i(t) - \alpha_i(t)), \end{aligned}$$

where $\chi_i(t)$ and $\hat{\chi}(t)$ lie between $\beta_i(t)$ and $\alpha_i(t)$. Therefore, we have

$$\begin{aligned} &- 2\sum_{i=1}^{n}\mathfrak{E}_{\mathfrak{R}i}(t)\Big(\mathfrak{A}_i(\beta_i(t))\mathfrak{g}_i(\beta_i(t)) \\ &- \mathfrak{A}_i(\alpha_i(t))\mathfrak{g}_i(\alpha_i(t))\Big) \\ &= -2\sum_{i=1}^{n}\mathfrak{E}_{\mathfrak{R}i}(t)\Big(\xi_i^{'}(\chi_i(t))\mathfrak{E}_i(t)\Big) \\ &\leq -2\sum_{i=1}^{n}\underline{\xi}_i|\mathfrak{E}_{\mathfrak{R}i}(t)||\mathfrak{E}_i(t)| \\ &\leq -\sum_{i=1}^{n}\underline{\xi}_i[\mathfrak{E}_{\mathfrak{R}i}^2(t) + \mathfrak{E}_i^2(t)]. \end{aligned} \tag{10}$$

Similarly,

$$\begin{aligned} &2\sum_{i=1}^{n}\mathfrak{E}_{\mathfrak{R}i}(t)\Big[\mathfrak{A}_i(\beta_i(t)) - \mathfrak{A}_i(\alpha_i(t))\Big]\mathfrak{I}_i(t) \\ &= -2\sum_{i=1}^{n}\mathfrak{E}_{\mathfrak{R}i}(t)\Big[\mathfrak{A}_i^{'}(\hat{\chi}_i(t))\mathfrak{E}_i(t)\mathfrak{I}_i(t)\Big] \\ &\leq -2\sum_{i=1}^{n}\lambda_i\tilde{l}_i|\mathfrak{E}_{\mathfrak{R}i}(t)||\mathfrak{E}_i(t)| \\ &\leq -\sum_{i=1}^{n}\lambda_i\tilde{l}_i\Big[\mathfrak{E}_{\mathfrak{R}i}^2(t) + \mathfrak{E}_i^2(t)\Big], \end{aligned} \tag{11}$$

and

$$\begin{aligned} &2\sum_{i=1}^{n}\mathfrak{E}_{\mathfrak{R}i}(t)\Big[-(\mathfrak{S}_i - 1)\mathfrak{E}_{\mathfrak{R}i}(t) \\ &- (1 - \mathfrak{S}_i)\mathfrak{E}_i(t)\Big] \\ &= -2\sum_{i=1}^{n}\mathfrak{E}_{\mathfrak{R}i}(t)(\mathfrak{S}_i - 1)\mathfrak{E}_{\mathfrak{R}i}(t) \end{aligned} \tag{12}$$

$$
\begin{aligned}
&- 2\sum_{i=1}^{n}\mathfrak{E}_{\Re i}(t)(1-\mathfrak{S}_i)\mathfrak{E}_i(t)\\
&\le -2\sum_{i=1}^{n}(|\mathfrak{S}_i-1|)\mathfrak{E}^2_{\Re i}(t)\\
&\quad -\sum_{i=1}^{n}(|1-\mathfrak{S}_i|)\Big[\mathfrak{E}^2_{\Re i}(t)+\mathfrak{E}^2_i(t)\Big].
\end{aligned}
$$

According to (H1)–(H2) and (H4), we obtain

$$
\begin{aligned}
&2\sum_{i=1}^{n}\mathfrak{E}_{\Re i}(t)\sum_{j=1}^{n}(\mathfrak{P}_{ij}+\Delta\mathfrak{P}_{ij})\times\\
&\Big[\mathfrak{A}_i(\beta_i(t))\mathfrak{f}_{1j}(\beta_j(t))-\mathfrak{A}_i(\alpha_i(t))\mathfrak{f}_{1j}(\alpha_j(t))\Big]\\
&=2\sum_{i=1}^{n}\mathfrak{E}_{\Re i}(t)\sum_{j=1}^{n}(\mathfrak{P}_{ij}+\Delta\mathfrak{P}_{ij})\times\\
&\quad\Big[\mathfrak{A}_i(\beta_i(t))\mathfrak{f}_{1j}(\beta_j(t))-\mathfrak{A}_i(\beta_i(t))\mathfrak{f}_{1j}(\alpha_j(t))\\
&\quad+\mathfrak{A}_i(\beta_i(t))\mathfrak{f}_{1j}(\alpha_j(t))-\mathfrak{A}_i(\alpha_i(t))\mathfrak{f}_{1j}(\alpha_j(t))\Big]\\
&=2\sum_{i=1}^{n}\mathfrak{E}_{\Re i}(t)\mathfrak{A}_i(\beta_i(t))\sum_{j=1}^{n}(\mathfrak{P}_{ij}+\Delta\mathfrak{P}_{ij})\times\\
&\quad\Big[\mathfrak{f}_{1j}(\beta_j(t))-\mathfrak{f}_{1j}(\alpha_j(t))\Big]\\
&+2\sum_{i=1}^{n}\mathfrak{E}_{\Re i}(t)(\mathfrak{A}_i(\beta_i(t))\\
&\quad-\mathfrak{A}_i(\alpha_i(t)))\sum_{j=1}^{n}(\mathfrak{P}_{ij}+\Delta\mathfrak{P}_{ij})\mathfrak{f}_{1j}(\alpha_j(t))\\
&\le 2\sum_{i=1}^{n}\sum_{j=1}^{n}\bar{\mathfrak{A}}_i(|\mathfrak{P}_{ij}|+\Lambda_{ij})\mathfrak{X}_j|\mathfrak{E}_{\Re i}(t)||\mathfrak{E}_i(t)|\\
&\quad+2\sum_{i=1}^{n}\sum_{j=1}^{n}2\bar{\mathfrak{A}}_i(|\mathfrak{P}_{ij}|+\Lambda_{ij})l_x|\mathfrak{E}_{\Re i}(t)|\\
&\le\sum_{i=1}^{n}\sum_{j=1}^{n}\bar{\mathfrak{A}}_i(|\mathfrak{P}_{ij}|+\Lambda_{ij})\mathfrak{X}_j\Big[\mathfrak{E}^2_{\Re i}(t)+\mathfrak{E}^2_i(t)\Big]\\
&\quad+2\sum_{i=1}^{n}\sum_{j=1}^{n}\Big[\mathfrak{E}^2_{\Re i}(t)+(\bar{\mathfrak{A}}_i(|\mathfrak{P}_{ij}|+\Lambda_{ij})l_x)^2\Big].
\end{aligned}
$$

Similarly,

$$
\begin{aligned}
&2\sum_{i=1}^{n}\mathfrak{E}_{\Re i}(t)\sum_{j=1}^{n}(\mathfrak{Q}_{ij}+\Delta\mathfrak{Q}_{ij})\Big[\mathfrak{A}_i(\beta_i(t))\times\\
&\mathfrak{f}_{2j}(\beta_j(t-\eta(t)))-\mathfrak{A}_i(\alpha_i(t))\mathfrak{f}_{2j}\\
&(\alpha_j(t-\eta(t)))\Big] \qquad (14)\\
&=2\sum_{i=1}^{n}\mathfrak{E}_{\Re i}(t)\sum_{j=1}^{n}(\mathfrak{Q}_{ij}+\Delta\mathfrak{Q}_{ij})\Big[\mathfrak{A}_i(\beta_i(t))\times\\
&\quad\mathfrak{f}_{2j}(\beta_j(t-\eta(t)))-\mathfrak{A}_i(\beta_i(t))\mathfrak{f}_{2j}(\alpha_j(t-\eta(t)))\\
&\quad+\mathfrak{A}_i(\beta_i(t))\mathfrak{f}_{2j}(\alpha_j(t-\eta(t)))\\
&\quad-\mathfrak{A}_i(\alpha_i(t))\mathfrak{f}_{2j}(\alpha_j(t-\eta(t)))\Big]\\
&=2\sum_{i=1}^{n}\mathfrak{E}_{\Re i}(t)\mathfrak{A}_i(\beta_i(t))\sum_{j=1}^{n}(\mathfrak{Q}_{ij}+\Delta\mathfrak{Q}_{ij})\\
&\quad\Big[\mathfrak{f}_{2j}(\beta_j(t-\eta(t)))-\mathfrak{f}_{2j}(\alpha_j(t-\eta(t)))\Big]\\
&\quad+2\sum_{i=1}^{n}\mathfrak{E}_{\Re i}(t)\Big[\mathfrak{A}_i(\beta_i(t))-\mathfrak{A}_i(\alpha_i(t))\Big]\times\\
&\quad\sum_{j=1}^{n}(\mathfrak{Q}_{ij}+\Delta\mathfrak{Q}_{ij})\mathfrak{f}_{2j}(\alpha_j(t-\eta(t)))\\
&\le 2\sum_{i=1}^{n}\sum_{j=1}^{n}\bar{\mathfrak{A}}_i(|\mathfrak{Q}_{ij}|+\Gamma_{ij})\mathfrak{Y}_j|\mathfrak{E}_{\Re i}(t)||\\
&\mathfrak{E}_i(t-\eta(t))|\\
&\quad+2\sum_{i=1}^{n}\sum_{j=1}^{n}2\bar{\mathfrak{A}}_i(|\mathfrak{Q}_{ij}|+\Gamma_{ij})l_\tau|\mathfrak{E}_{\Re i}(t)|\\
&\le\sum_{i=1}^{n}\sum_{j=1}^{n}\bar{\mathfrak{A}}_i(|\mathfrak{Q}_{ij}|+\Gamma_{ij})\mathfrak{Y}_j\Big[\mathfrak{E}^2_{\Re i}(t)\\
&+\mathfrak{E}^2_i(t-\eta(t))\Big]\\
&\quad+2\sum_{i=1}^{n}\sum_{j=1}^{n}\Big[\mathfrak{E}^2_{\Re i}(t)+(\bar{\mathfrak{A}}_i(|\mathfrak{Q}_{ij}|+\Gamma_{ij})l_\tau)^2\Big]
\end{aligned}
$$

and

$$
\begin{aligned}
&- 2\sum_{i=1}^{n}\mathfrak{E}_{\Re i}(t)(\mathfrak{K}_{1i}\mathfrak{E}_i(t)+\mathfrak{K}_{2i}\mathfrak{E}_{\Re i}(t))\\
&\le -2\sum_{i=1}^{n}\mathfrak{K}_{ai}|\mathfrak{E}_{\Re i}(t)||\mathfrak{E}_i(t)|\\
&\quad-2\sum_{i=1}^{n}\mathfrak{K}_{bi}|\mathfrak{E}_{\Re i}(t)||\mathfrak{E}_{\Re i}(t)| \qquad (15)\\
&\le -\sum_{i=1}^{n}\mathfrak{K}_{ai}\Big[\mathfrak{E}^2_{\Re i}(t)+\mathfrak{E}^2_i(t)\Big]\\
&\quad-2\sum_{i=1}^{n}\mathfrak{K}_{bi}\mathfrak{E}^2_{\Re i}(t).
\end{aligned}
$$

In (9), substituting (10)–(15), we obtain

$$
\begin{aligned}
&{}_0\mathcal{D}^{\phi}_t\mathfrak{V}(t)\\
&\quad=-\sum_{i=1}^{n}\{\underline{\xi}_i+2+\lambda_i\tilde{l}_i+|\mathfrak{S}_i|\\
&\quad-\sum_{j=1}^{n}\bar{\mathfrak{A}}_i(|\mathfrak{P}_{ij}
\end{aligned}
$$

$$
\begin{aligned}
&+\Lambda_{ij}|)\mathfrak{X}_j+\mathfrak{K}_{ai}\}\mathfrak{E}_i^2(t)\\
&-\sum_{i=1}^{n}\{\underline{\xi}_i+\lambda_i\tilde{l}_i+3|\mathfrak{S}_i|\\
&-4-4n+\mathfrak{K}_{ai}+2\mathfrak{K}_{bi}\\
&-\sum_{j=1}^{n}\big[\bar{\mathfrak{A}}_i(|\mathfrak{P}_{ij}+\Lambda_{ij}|)\mathfrak{X}_j\\
&-\bar{\mathfrak{A}}_i(|\mathfrak{Q}_{ij}+\Gamma_{ij}|)\mathfrak{Y}_j\big]\}\mathfrak{E}_{\Re i}(t)\\
&+\sum_{i=1}^{n}\sum_{j=1}^{n}\bar{\mathfrak{A}}_i(|\mathfrak{Q}_{ij}+\Gamma_{ij}|)\mathfrak{Y}_j\mathfrak{E}_i^2(t-\eta(t))\\
&+\sum_{i=1}^{n}\sum_{j=1}^{n}\Big[(\bar{\mathfrak{A}}_i(|\mathfrak{P}_{ij}+\Lambda_{ij}|)l_x)^2\\
&\quad+(\bar{\mathfrak{A}}_i(|\mathfrak{Q}_{ij}+\Gamma_{ij}|)l_\tau)^2\Big]\\
&\le-\mathfrak{I}_1\sum_{i=1}^{n}\mathfrak{E}_i^2(t)-\mathfrak{I}_2\sum_{i=1}^{n}\mathfrak{E}_{\Re i}^2(t)\\
&+\mathfrak{I}_b\sum_{i=1}^{n}\mathfrak{E}_i^2(t-\eta(t))+\mathfrak{I}_c
\end{aligned}
$$

where

$$
\begin{aligned}
\mathfrak{I}_1=&\min_{1\le i\le n}\{\underline{\xi}_i+2+\lambda_i\tilde{l}_i+|\mathfrak{S}_i|\\
&-\sum_{j=1}^{n}\bar{\mathfrak{A}}_i(|\mathfrak{P}_{ij}+\Lambda_{ij}|)\mathfrak{X}_j+\mathfrak{K}_{ai}\},\\
\mathfrak{I}_2=&\min_{1\le i\le n}\{\underline{\xi}_i+\lambda_i\tilde{l}_i+3|\mathfrak{S}_i|-4-4n\\
&+\mathfrak{K}_{ai}+2\mathfrak{K}_{bi}\\
&-\sum_{j=1}^{n}\big[\bar{\mathfrak{A}}_i(|\mathfrak{P}_{ij}\\
&+\Lambda_{ij}|)\mathfrak{X}_j-\bar{\mathfrak{A}}_i(|\mathfrak{Q}_{ij}+\Gamma_{ij}|)\mathfrak{Y}_j\},
\end{aligned}
$$

$$
\begin{aligned}
\mathfrak{I}_b=&\max_{1\le i\le n}\{\bar{\mathfrak{A}}_i(|\mathfrak{Q}_{ij}+\Gamma_{ij}|)\mathfrak{Y}_j\},\\
\mathfrak{I}_c=&\sum_{i=1}^{n}\sum_{j=1}^{n}\Big[(\bar{\mathfrak{A}}_i(|\mathfrak{P}_{ij}+\Lambda_{ij}|)l_x)^2\\
&+(\bar{\mathfrak{A}}_i(|\mathfrak{Q}_{ij}+\Gamma_{ij}|)l_\tau)^2\big],\\
\mathfrak{I}_a=&min(\mathfrak{I}_1,\mathfrak{I}_2).
\end{aligned}
$$

Applying the fractional-order Razumikhin technique, we obtain

$$
\begin{aligned}
{}_0\mathcal{D}_t^{\phi}\mathfrak{V}(t)\le&-\mathfrak{I}_a\mathfrak{V}(t)+\mathfrak{I}_b\\
&\max_{t-\eta(t)\le s\le t}\mathfrak{V}(s)+\mathfrak{I}_c.
\end{aligned}\tag{16}
$$

By using Lemma 3, we have

$$
\mathfrak{V}(t)\le\mathfrak{M}\mathcal{E}_\phi(-\theta t^\phi)+\frac{\mathfrak{I}_c}{\mathfrak{I}_a-\mathfrak{I}_b},
$$

where

$$
\theta=\sup_{t-\eta(t)\ge1}\{\hat{\theta}|\hat{\theta}-\mathfrak{I}_a-\mathfrak{I}_b\frac{\mathcal{E}_\phi(\hat{\theta}(t-\eta(t))^\phi)}{\mathcal{E}_\phi(\hat{\theta}t^\phi)}=0\}.
$$

From this we obtain

$$
\begin{aligned}
\|\mathfrak{E}(t)\|\le&\|\mathfrak{E}(t)\|+\|\mathfrak{E}_{\Re}(t)\|\\
\le&\{\mathfrak{M}\mathcal{E}_\phi(\theta t^\phi)\}^{\frac{1}{2}}+\frac{\sqrt{\mathfrak{I}_c}}{\sqrt{\mathfrak{I}_a-\mathfrak{I}_b}},
\end{aligned}
$$

which confirms that system (1) achieves QML synchronization with system (2), with convergence rate θ and error bound $\frac{\sqrt{\mathfrak{I}_c}}{\sqrt{\mathfrak{I}_a-\mathfrak{I}_b}}$.

4.2. Adaptive controller

However, selecting the controller gains $\mathcal{K}_{ai}$ and $\mathcal{K}_{bi}$ in controller (6) is challenging, as they must be chosen sufficiently large to satisfy condition (7), which may lead to a conservative design, especially when dealing with uncertain systems. So to overcome this limitation in this section, we adopt the adaptive controller, which can tune its gain automatically to enhance the system performance. The adaptive controller for the system (5) is constructed as

$$
\begin{aligned}
&\mathfrak{U}_i(t)=\mathfrak{K}_{ai}(t)\mathfrak{E}_{\Re i}(t)+\mathfrak{K}_{bi}(t)\mathfrak{E}_i(t)\,\mathrm{sign}(\mathfrak{E}_{\Re i}(t)),\\
&{}_0\mathcal{D}_t^{\phi}\mathfrak{K}_{ai}(t)=-\pi_{ai}\mathfrak{E}_{\Re i}^2(t),\\
&{}_0\mathcal{D}_t^{\phi}\mathfrak{K}_{bi}(t)=-\pi_{bi}|\mathfrak{E}_i(t)||\mathfrak{E}_{\Re i}(t)|,
\end{aligned}\tag{17}
$$

where $\pi_{ai}>0$ and $\pi_{bi}>0$.

Theorem 2. *Under the hypotheses (H1)-(H4), if there exist constants π_{ai} and π_{bi} such that*

$$
\begin{cases}
\beth_a:=min(\beth_1,\beth_2)\ge0,\\
\beth_b:=\max_{1\le i\le n}\{\bar{\mathfrak{A}}_i(|\mathfrak{Q}_{ij}+\Gamma_{ij}|)\mathfrak{Y}_j\},\\
\beth_c:=\sum_{i=1}^{n}\sum_{j=1}^{n}\Big[(\bar{\mathfrak{A}}_i(|\mathfrak{P}_{ij}+\Lambda_{ij}|)l_x)^2\\
+(\bar{\mathfrak{A}}_i(|\mathfrak{Q}_{ij}+\Gamma_{ij}|)l_\tau)^2\big]\ge0,
\end{cases}\tag{18}
$$

where

$$
\begin{aligned}
\beth_1=&\min_{1\le i\le n}\{\underline{\xi}_i+2+\lambda_i\tilde{l}_i+|\mathfrak{S}_i|+\mathfrak{K}_b^*\\
&-\sum_{j=1}^{n}\bar{\mathfrak{A}}_i(|\mathfrak{P}_{ij}+\Lambda_{ij}|)\mathfrak{X}_j\},\\
\beth_2=&\min_{1\le i\le n}\{\underline{\xi}_i+\lambda_i\tilde{l}_i+3|\mathfrak{S}_i|-4-4n\\
&+2\mathfrak{K}_a^*+\mathfrak{K}_b^*\\
&-\sum_{j=1}^{n}\big[\bar{\mathfrak{A}}_i(|\mathfrak{P}_{ij}+\Lambda_{ij}|)\mathfrak{X}_j-\bar{\mathfrak{A}}_i(|\mathfrak{Q}_{ij}\\
&+\Gamma_{ij}|)\mathfrak{Y}_j\},\\
\beth_b=&\max_{1\le i\le n}\{\bar{\mathfrak{A}}_i(|\mathfrak{Q}_{ij}+\Gamma_{ij}|)\mathfrak{Y}_j\},\\
\beth_c=&\sum_{i=1}^{n}\sum_{j=1}^{n}\Big[(\bar{\mathfrak{A}}_i(|\mathfrak{P}_{ij}+\Lambda_{ij}|)l_x)^2\\
&+(\bar{\mathfrak{A}}_i(|\mathfrak{Q}_{ij}+\Gamma_{ij}|)l_\tau)^2\big],\\
\beth_a=&min(\beth_1,\beth_2),
\end{aligned}
$$

then system (1) can achieve the QML synchronization with the system (2) under the controller (17) with an error bound $\sqrt{\frac{\beth_c}{\beth_a-\beth_b}}$.

Proof. Let's consider the Lyapunov function as

$$\mathfrak{V}_2(t) = \mathfrak{V}_a(t) + \mathfrak{V}_b(t), \tag{19}$$

where

$$\mathfrak{V}_a(t) = \sum_{i=1}^{n} \mathfrak{E}_i^2(t) + \sum_{i=1}^{n} \mathfrak{E}_{\Re i}^2(t),$$

$$\mathfrak{V}_b(t) = \sum_{i=1}^{n} \frac{1}{\pi_{ai}}(\mathfrak{K}_{ai}(t) - \mathfrak{K}_a^*)^2 + \sum_{i=1}^{n} \frac{1}{\pi_{bi}}(\mathfrak{K}_{bi}(t) - \mathfrak{K}_b^*)^2.$$

By computing the fractional derivative of $\mathfrak{V}_a(t)$ according Lemma 2 along (5), we obtain

$$\begin{aligned}
&{}_0\mathcal{D}_t^{\phi}\mathfrak{V}_a(t)\\
&\le 2\sum_{i=1}^{n} \mathfrak{E}_i(t)\,{}_0\mathcal{D}_t^{\phi}\mathfrak{E}_i(t) + 2\sum_{i=1}^{n} \mathfrak{E}_{\Re i}(t)\,{}_0\mathcal{D}_t^{\phi}\mathfrak{E}_{\Re i}(t)\\
&\le 2\sum_{i=1}^{n} \mathfrak{E}_i(t)\Big[\mathfrak{E}_{\Re i}(t) - \mathfrak{E}_i(t)\Big] + 2\sum_{i=1}^{n} \mathfrak{E}_{\Re i}(t)\times\\
&\Big[-(\mathfrak{S}_i - 1)\mathfrak{E}_{\Re i}(t) - (1-\mathfrak{S}_i)\mathfrak{E}_i(t)\\
&- \mathfrak{A}_i(\beta_i(t))\mathfrak{g}_i(\beta_i(t)) + \mathfrak{A}_i(\alpha_i(t))\mathfrak{g}_i(\alpha_i(t))\\
&+ \mathfrak{A}_i(\beta_i(t))\sum_{j=1}^{n}(\mathfrak{P}_{ij} + \Delta\mathfrak{P}_{ij})\mathfrak{f}_{1j}(\beta_j(t))\\
&- \mathfrak{A}_i(\alpha_i(t))\sum_{j=1}^{n}(\mathfrak{P}_{ij} + \Delta\mathfrak{P}_{ij})\mathfrak{f}_{1j}(\alpha_j(t))\\
&+ \mathfrak{A}_i(\beta_i(t))\sum_{j=1}^{n}(\mathfrak{Q}_{ij} + \Delta\mathfrak{Q}_{ij})\mathfrak{f}_{1j}(\beta_j(t-\eta(t)))\\
&+ \mathfrak{A}_i(\alpha_i(t))\sum_{j=1}^{n}(\mathfrak{Q}_{ij} + \Delta\mathfrak{Q}_{ij})\mathfrak{f}_{1j}(\alpha_j(t-\eta(t)))\\
&+ \mathfrak{A}_i(\beta_i(t))\mathfrak{I}_i(t) - \mathfrak{A}_i(\beta_i(t))\mathfrak{I}_i(t)\\
&+ \mathfrak{K}_{ai}(t)\mathfrak{E}_{\Re i}(t)\\
&+ \mathfrak{K}_{bi}|\mathfrak{E}_i(t)|sign(\mathfrak{E}_{\Re i}(t))\Big].
\end{aligned} \tag{20}$$

The fractional derivative of $\mathfrak{V}_b(t)$ is

$$\begin{aligned}
{}_0\mathcal{D}_t^{\phi}\mathfrak{V}_b(t) &\le -2\sum_{i=1}^{n}(\mathfrak{K}_{ai}(t) - \mathfrak{K}_a^*)\mathfrak{E}_{\Re i}^2(t)\\
&- 2\sum_{i=1}^{n}(\mathfrak{K}_{ai}(t) - \mathfrak{K}_b^*)|\mathfrak{E}_i(t)||\mathfrak{E}_{\Re i}(t)|.
\end{aligned} \tag{21}$$

From (20) and (21) we derive ${}_0\mathcal{D}_t^{\phi}\mathfrak{V}_2(t)$. The remaining steps are similar to Theorem 1. Therefore, we obtain

$$\begin{aligned}
{}_0\mathcal{D}_t^{\phi}\mathfrak{V}_2(t) &= {}_0\mathcal{D}_t^{\phi}\mathfrak{V}_a(t) + {}_0\mathcal{D}_t^{\phi}\mathfrak{V}_b(t)\\
&\le -\sum_{i=1}^{n}\{\underline{\xi}_i + 2 + \lambda_i\tilde{l}_i + |\mathfrak{S}_i| + \mathfrak{K}_b^*\\
&- \sum_{j=1}^{n}\bar{\mathfrak{A}}_i(|\mathfrak{P}_{ij} + \Lambda_{ij}|)\mathfrak{X}_j\}\mathfrak{E}_i^2(t)\\
&- \sum_{i=1}^{n}\{\underline{\xi}_i + \lambda_i\tilde{l}_i\\
&+ 3|\mathfrak{S}_i| - 4 - 4n + 2\mathfrak{K}_a^* + \mathfrak{K}_b^*\\
&- \sum_{j=1}^{n}\big[\bar{\mathfrak{A}}_i(|\mathfrak{P}_{ij} + \Lambda_{ij}|)\mathfrak{X}_j\\
&- \bar{\mathfrak{A}}_i(|\mathfrak{Q}_{ij} + \Gamma_{ij}|)\mathfrak{Y}_j\big]\}\mathfrak{E}_{\Re i}(t)\\
&+ \sum_{i=1}^{n}\sum_{j=1}^{n}\bar{\mathfrak{A}}_i(|\mathfrak{Q}_{ij} + \Gamma_{ij}|)\mathfrak{Y}_j\mathfrak{E}_i^2(t-\eta(t))\\
&+ \sum_{i=1}^{n}\sum_{j=1}^{n}\Big[(\bar{\mathfrak{A}}_i(|\mathfrak{P}_{ij} + \Lambda_{ij}|)l_x)^2\\
&+ (\bar{\mathfrak{A}}_i(|\mathfrak{Q}_{ij} + \Gamma_{ij}|)l_\tau)^2\Big]\\
&\le -\beth_1\sum_{i=1}^{n}\mathfrak{E}_i^2(t) - \beth_2\sum_{i=1}^{n}\mathfrak{E}_{\Re i}^2(t)\\
&+ \beth_b\sum_{i=1}^{n}\mathfrak{E}_i^2(t-\eta(t)) + \beth_c
\end{aligned}$$

where

$$\begin{aligned}
\beth_1 &= \min_{1\le i\le n}\{\underline{\xi}_i + 2 + \lambda_i\tilde{l}_i + |\mathfrak{S}_i| + \mathfrak{K}_b^*\\
&\quad - \sum_{j=1}^{n}\bar{\mathfrak{A}}_i(|\mathfrak{P}_{ij} + \Lambda_{ij}|)\mathfrak{X}_j\},\\
\beth_2 &= \min_{1\le i\le n}\{\underline{\xi}_i + \lambda_i\tilde{l}_i + 3|\mathfrak{S}_i| - 4\\
&\quad - 4n + 2\mathfrak{K}_a^* + \mathfrak{K}_b^*\\
&\quad - \sum_{j=1}^{n}\big[\bar{\mathfrak{A}}_i(|\mathfrak{P}_{ij} + \Lambda_{ij}|)\mathfrak{X}_j\\
&\quad - \bar{\mathfrak{A}}_i(|\mathfrak{Q}_{ij} + \Gamma_{ij}|)\mathfrak{Y}_j\},\\
\beth_b &= \max_{1\le i\le n}\{\bar{\mathfrak{A}}_i(|\mathfrak{Q}_{ij} + \Gamma_{ij}|)\mathfrak{Y}_j\},\\
\beth_c &= \sum_{i=1}^{n}\sum_{j=1}^{n}\Big[(\bar{\mathfrak{A}}_i(|\mathfrak{P}_{ij} + \Lambda_{ij}|)l_x)^2\\
&\quad + (\bar{\mathfrak{A}}_i(|\mathfrak{Q}_{ij} + \Gamma_{ij}|)l_\tau)^2\big],\\
\beth_a &= min(\beth_1, \beth_2),
\end{aligned}$$

Applying the fractional-order Razumikhin technique, we obtain

$$\begin{aligned}
{}_0\mathcal{D}_t^{\phi}\mathfrak{V}_2(t) &\le -\beth_a\mathfrak{V}(t) + \beth_b\\
&\sup_{t-\eta(t)\le s\le t}\mathfrak{V}(s) + \beth_c.
\end{aligned} \tag{22}$$

By Lemma 2 and for any $\mathcal{W} > 0$,

$$\mathfrak{V}_2(t) \leq \frac{\left(\mathfrak{V}_a(0)+\mathfrak{V}_b(0)-\frac{\beth_c}{\beth_a}\right)\mathcal{E}_\phi(-\beth_a t^\phi)+\frac{\beth_c}{\beth_a}}{1-\frac{\beth_b}{\beth_a}}+\mathcal{W}.$$

Consequently, taking $\mathcal{W}\to 0$, we obtain

$$\begin{aligned}\|\mathfrak{E}(t)\| \leq & \|\mathfrak{E}(t)\|+\|\mathfrak{E}_{\Re}(t)\| \\ \leq & \{\mathcal{W}_\nu \mathfrak{E}_\phi(-\beth_a t^\phi)\}^{\frac{1}{2}}+\sqrt{\frac{\beth_c}{\beth_a-\beth_b}}\end{aligned}$$

where $\mathcal{W}_\nu = \frac{\left(\mathfrak{V}_a(0)+\mathfrak{V}_b(0)-\frac{\beth_c}{\beth_a}\right)}{1-\frac{\beth_b}{\beth_a}}$, which confirms that system (1) achieves QML synchronization with system (2), with convergence rate θ and error bound $\frac{\sqrt{\beth_c}}{\sqrt{\beth_a-\beth_b}}$. □

5. Numerical simulation

Example 1. *Consider the 2-D delayed FOCGINN systems (1) and (2) with the following parameters:*
$\phi = 0.98, \Delta\mathfrak{P}_{ij} = \Delta\mathfrak{Q}_{ij} = 0.1\cos(t), i,j = 1,2.$

$$\mathfrak{S} = \begin{bmatrix} 1.1 & 0 \\ 0 & 1.1 \end{bmatrix},\quad \mathfrak{P} = \begin{bmatrix} 1.3 & 1.2 \\ 1.1 & -1.2 \end{bmatrix} \text{ and}$$

$$\mathfrak{Q} = \begin{bmatrix} 1.2 & -1.5 \\ -1.5 & 1.5 \end{bmatrix}.$$

The functions in the systems are $\mathfrak{A}_i(\alpha_i(t)) = 0.4\alpha_i(t), = \mathfrak{A}_i(\beta_i(t)) = 0.4\beta_i(t), \mathfrak{g}_i(\alpha_i(t)) = 0.3[1+\frac{1}{1+|\alpha_i(t)|}], \mathfrak{g}_i(\beta_i(t)) = 0.3[1+\frac{1}{1+|\beta_i(t)|}], \mathfrak{f}_{1j}(\cdot) = \mathfrak{f}_{2j}(\cdot) = 0.5\tanh(\cdot)$ *and* $\mathfrak{I}_i(t) = 0$. *With the initial conditions* $\alpha_1(0) = 0.2, \alpha_2(0) = -1.1, \beta_1(0) = -0.3$, *and* $\beta_2(0) = -1.8$, *the phase trajectories of system (1) are displayed in* ***Figure 1****. From hypotheses (H1)-(H2), we obtain the following values by calculation:* $\underline{\mathfrak{A}}_i = \bar{\mathfrak{A}}_i = 0.9, \lambda_i = 0.3, \xi_i = 0.18, \mathfrak{X}_i = \mathfrak{Y}_i = l_i^x = l_i^\tau = \tilde{l}_i = 1, i = 1,2.$

The controller parameters are adopted as $\mathfrak{K}_{ai} = 2.6, \mathfrak{K}_{bi} = 2.6$. *With the help of controller (6) and the conditions of Theorem 1, we obtain the synchronization error bound as* $\frac{\sqrt{\beth_c}}{\sqrt{\beth_a-\beth_b}} = 0.9571$. *These results show that systems (1) and (2) achieve QML synchronization.* ***Figures 2*** *and* ***3*** *show the state behavior of systems (1) and (2) under controller (6), and* ***Figure 4*** *shows the synchronization error together with the actual and theoretical bounds.*

Example 2. *Consider the 3-D delayed FOCGINN system with the following parameters:* $\phi = 0.88, \mathfrak{S} = diag(1.01, 1.01, 1.01), \Delta\mathfrak{P}_{ij} = \mathfrak{Q}_{ij} = 0.3\cos(t), i,j = 1,2.$

$$\mathfrak{P} = \begin{bmatrix} 1.3 & 0.2 & 1.4 \\ -0.9 & -1.2 & 1.1 \\ 1.1 & -1.2 & 1.1 \end{bmatrix},$$

$$\mathfrak{Q} = \begin{bmatrix} 1.2 & -1.5 & 2.1 \\ -1.5 & 1.5 & 1.1 \\ 2.1 & 1.1 & 1.1 \end{bmatrix}$$

The functions inthe systems are $\mathfrak{A}_i(\alpha_i(t)) = 0.4\alpha_i(t), \mathfrak{A}_i(\beta_i(t)) = 0.4\beta_i(t), \mathfrak{g}_i(\alpha_i(t)) = 0.4[2+\frac{1}{1+|\alpha_i(t)|}], \mathfrak{g}_i(\beta_i(t)) = 0.4[2+\frac{1}{1+|\beta_i(t)|}], \mathfrak{f}_{1j}(\cdot) = \mathfrak{f}_{2j}(\cdot) = 0.5\tanh(\cdot), \eta(t) = 0.3+(sin(2.9t))$ *and* $\mathfrak{I}_i(t) = 0$. *With the initial conditions* $\alpha_1(0), = 0.2, \alpha_2(0) = 1.4, \alpha_3(0) = 0.1, \beta_1(0) = -0.3, \beta_2(0) = 1.6$, *and* $\beta_3(0) = 1.1$, *the phase trajectories of system (1) are displayed in* ***Figure 5****. From hypotheses (H1)-(H4), we obtain the following parameters by calculation:* $\underline{\mathfrak{A}}_i = \bar{\mathfrak{A}}_i = 0.9, \lambda_i = 0.3, \xi_i = 0.18, \mathfrak{X}_i = \mathfrak{Y}_i = l_i^x = l_i^\tau = \tilde{l}_i = 1, i = 1,2,3.$ *This example relies on Theorem 2. The adaptive controller (17) is employed, and the control parameters are selected according to the adaptive law as* $\pi_{a1} = 4.2, \pi_{a2} = 4.2, \pi_{a3} = 4.2, \pi_{b1} = 2.1, \pi_{b2} = 2.3, \pi_{b3} = 4.2$. *Based on the controller (17), systems (1) and (2) attain QML synchronization with the error bound* $\frac{\sqrt{\beth_c}}{\sqrt{\beth_a-\beth_b}} = 0.6757$. ***Figures 6–8*** *depict the state responses of systems (1) and (2) in the presence of adaptive controller (17), and the synchronization error bound is displayed in* ***Figure 9****. The adaptive gain trajectories are illustrated in* ***Figures 10*** *and* ***11****.*

Table 2 compares the synchronization error bounds of system (5) based on the proposed controllers. The adaptive controller reduces the theoretical and actual error bounds by 29.4% and 83.8%, respectively, compared with the state-feedback controller, indicating improved synchronization accuracy.

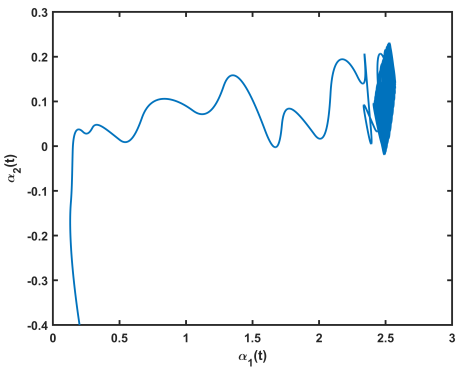


Figure 1. Phase trajectories of system (1)

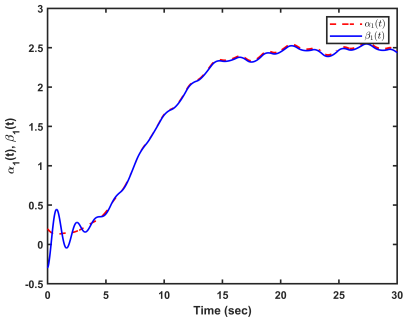


Figure 2. Time responses of the drive and response systems under controller (6)

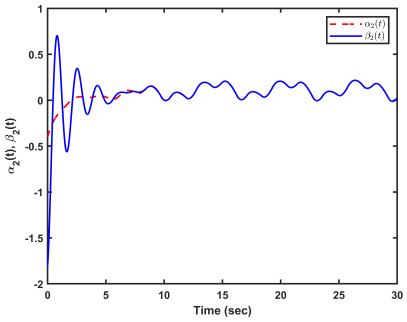


Figure 3. Time responses of the drive and response systems under controller (6)

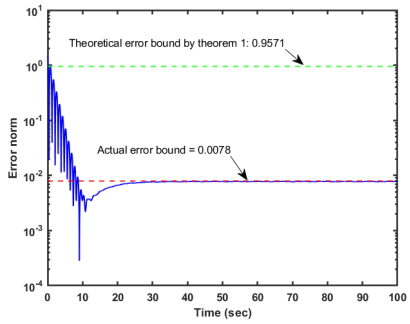


Figure 4. Time evolution of $\|\mathfrak{E}(t)\|$ under controller (6)

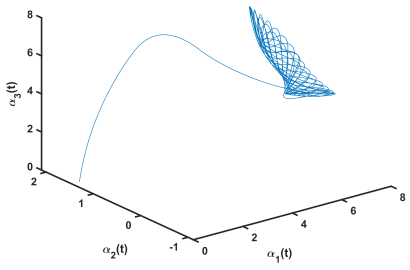


Figure 5. Phase trajectories of system (1)

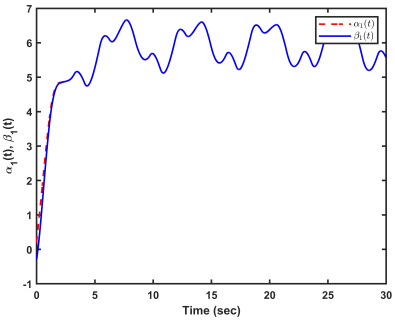


Figure 6. Time responses of the drive and response systems under controller (17)

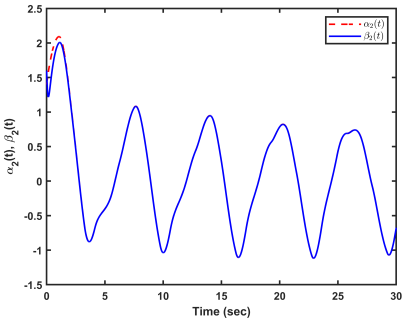


Figure 7. Time responses of the drive and response systems under controller (17)

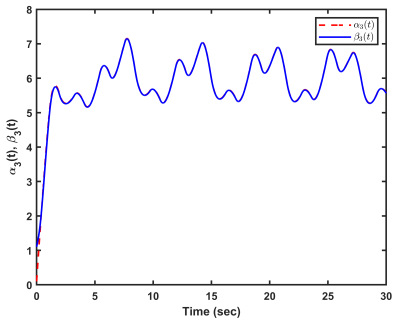


Figure 8. Time responses of the drive and response systems under controller (17)

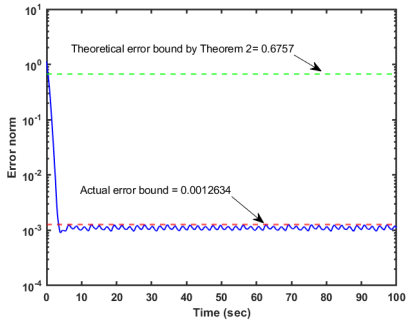


Figure 9. Time evolution of $\|\mathfrak{E}(t)\|$ under controller (17)

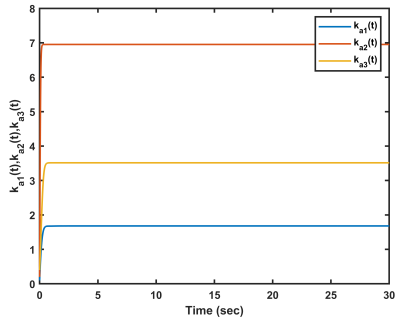


Figure 10. Time responses of the adaptive gains $\mathfrak{K}_{ai}, (i = 1, 2, 3)$

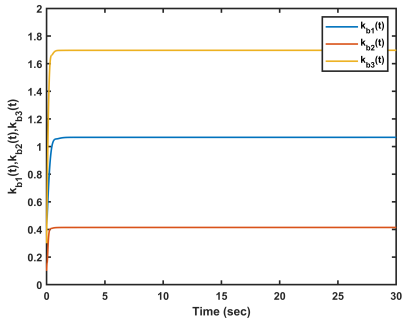


Figure 11. Time responses of the adaptive gains $\mathfrak{K}_{bi}, (i = 1, 2, 3)$

Table 2. Comparison of the proposed controllers based on error bounds

Proposed controllers	Theoretical error bound	Actual error bound
(6)	0.9571	0.0078
(17)	0.6757	0.0012634
Reduction using adaptive controller (%)	29.4%	83.8%

Example 3. *Consider the 2-D delayed FOCGINN systems (1) and (2) with the following parameters:* $\Delta\mathfrak{P}_{ij} = \Delta\mathfrak{Q}_{ij} = 0.5\sin(t)$,

$$\mathfrak{S} = \begin{bmatrix} 1.01 & 0 \\ 0 & 1.01 \end{bmatrix}, \quad \mathfrak{P} = \begin{bmatrix} 3.3 & 0.2 \\ -0.9 & -1.2 \end{bmatrix},$$

$$\mathfrak{Q} = \begin{bmatrix} 2.2 & -1.5 \\ -1.5 & 1.5 \end{bmatrix}$$

The functions in the systems are $\mathfrak{A}_i(\alpha_i(t)) = 0.2\alpha_i(t), = \mathfrak{A}_i(\beta_i(t)) = 0.2\beta_i(t), \mathfrak{g}_i(\alpha_i(t)) = 0.5[2 + \frac{1}{1+|\alpha_i(t)|}], \mathfrak{g}_i(\beta_i(t)) = 0.5[2 + \frac{1}{1+|\beta_i(t)|}], \mathfrak{f}_{1j}(\cdot) = \mathfrak{f}_{2j}(\cdot) = 0.5\tanh(\cdot), \mathfrak{I}_i(t) = 0$ *and* $\eta(t) = \frac{e^t}{e^T+1}$. *The initial conditions are* $\alpha_1(0) = 0.2, \alpha_2(0) = -1.1, \beta_1(0) = -0.3$, *and* $\beta_2(0) = -1.8$. *Then, the phase trajectories of the delayed FOCGINNs are depicted in* ***Figures 12–14*** *for different fractional orders. For the fractional order* $\phi = 0.77$, *from hypotheses (H1)-(H4), we obtain the following parameters by calculation:* $\underline{\mathfrak{A}}_i = \bar{\mathfrak{A}}_i = 0.6, \lambda_i = 0.5, \xi_i = 0.38, \mathfrak{X}_i = \mathfrak{Y}_i = l_i^x = l_i^\tau = \tilde{l}_i = 1, i = 1, 2$. *This example relies on Theorem 2. We employ adaptive controller (17) and choose the control parameters according to the adaptive law as* $\pi_{a1} = 2.2, \pi_{a2} = 2.2, \pi_{b1} = 4.1, \pi_{b2} = 4.3$. *Using controller (17), systems (1) and (2) attain QML synchronization.* ***Figures 15*** *and* ***16*** *depict the state response of the systems (1) and (2) under the presence of the adaptive controller (17), and its synchronization error bound is displayed in* ***Figure 17***. ***Table 3*** *compares the error-state convergence times of the proposed synchronization scheme with existing literature models.*

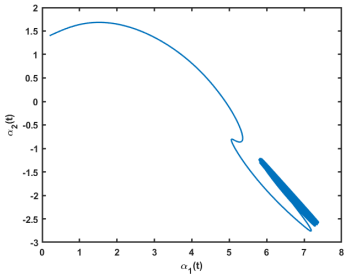


Figure 12. Phase trajectories of system (1) for $\phi = 0.77$

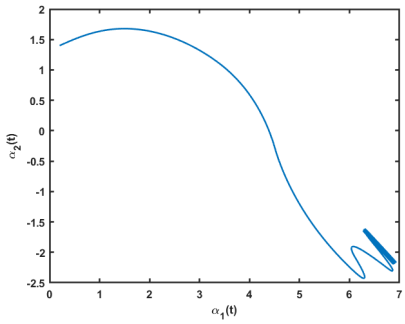


Figure 13. Phase trajectories of system (1) for $\phi = 0.88$

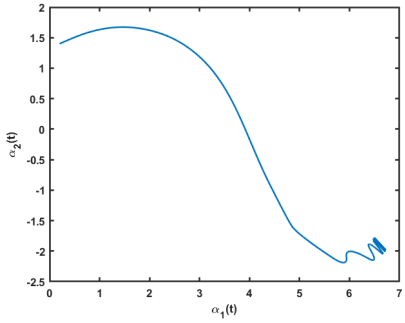


Figure 14. Phase trajectories of system (1) for $\phi = 0.99$

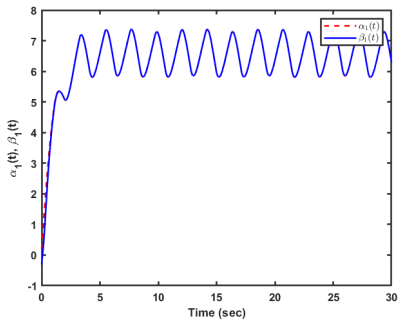


Figure 15. Time responses of the drive and response systems under controller (17)

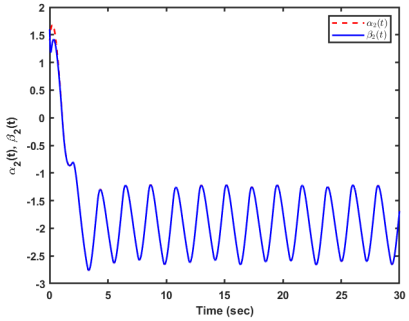


Figure 16. Time responses of the drive and response systems under controller (17)

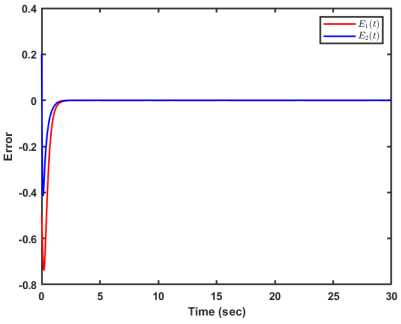


Figure 17. Synchronization error in Example 3

Table 3. Comparison of convergence times

Method	Convergence time (s)
[37]	5
[45]	4
Proposed	3.02

6. Conclusion

This work addressed the QML synchronization analysis of delayed FOCGINNs with uncertain parameters. The FOCGINN was successfully converted into an equivalent standard FOCGNN by applying an appropriate variable transformation. To attain QML synchronization, two control approaches, namely, a state-feedback controller and an adaptive controller, were proposed and implemented. Based on these controllers, using Lyapunov stability theory and the proposed lemmas, sufficient conditions for attaining QML synchronization were established through two theorems. To highlight the applicability of the derived outcomes, numerical simulation examples were presented. However, the present study is limited to theoretical synchronization analysis and numerical validation, without considering practical engineering implementation or experimental validation. As a future direction, the proposed synchronization framework will be extended to secure communication applications, with particular emphasis on developing an application-oriented encryption scheme based on synchronized neural dynamics.

Acknowledgments

None.

Funding

Open access funding provided by Vellore Institute of Technology.

Conflict of interest

The authors declare they have no competing interests.

Author contributions

Conceptualization: Pavithra Ganeshan, Dharani Shanmugavel
Formal analysis: Pavithra Ganeshan, Dharani Shanmugavel
Investigation: Pavithra Ganeshan
Methodology: Dharani Shanmugavel
Supervision: Dharani Shanmugavel
Validation: Sivakumar Muthusamy
Visualization: Sivakumar Muthusamy
Writing-original draft: Pavithra Ganeshan
Writing-review & editing: Dharani Shanmugavel, Sivakumar Muthusamy

Availability of data

Not applicable.

AI tools statement

All authors confirm that no AI tools were used in the preparation of this manuscript.

References

1. Liu J, Gong M, He H. Deep associative neural network for associative memory based on unsupervised representation learning. *Neural Netw.* 2019;113:41-53. https://doi.org/10.1016/j.neunet.2019.01.004
2. Abiodun OI, Jantan A, Omolara AE, *et al.* Comprehensive review of artificial neural network applications to pattern recognition. *IEEE Access.* 2019;7:158820-158846. https://doi.org/10.1109/ACCESS.2019.2945545
3. Mani P, Rajan R, Shanmugam L, Joo YH. Adaptive control for fractional order induced chaotic fuzzy cellular neural networks and its application to image encryption. *Inf Sci.* 2019;491:74-89. https://doi.org/10.1016/j.ins.2019.04.007
4. Chen J, Xiao M, Wu X, *et al.* Stability switching and oscillation regulation strategies for large-scale fractional-order neural networks with double hubs and multiple delays. *IEEE Trans Cybern.* 2026. https://doi.org/10.1109/TCYB.2026.3695452
5. Solouma E, Alsulami M, Baskonus HM, Aljohani AF, Saber S. On the stochastic simulation by optimal control and bifurcation analysis of the computer virus model in Caputo-type. *Alex Eng J.* 2026;144:12-22. https://doi.org/10.1016/j.aej.2026.04.017
6. Almalki FMK, Solouma E, Yavuz M, Saber S, Sarrah A. Analytical and numerical study of bifurcations and reaction-diffusion patterns in a predator-prey model with Holling-III response and variable carrying capacity. *Ain Shams Eng J.* 2026;17(6):104131. https://doi.org/10.1016/j.asej.2026.104131
7. Jacob J, Dharani S. Projective lag synchronization for quaternion neural networks with semi-Markov switching and mixed delays via non-fragile sliding mode control. *Syst Sci Control Eng.* 2025;13(1):2600780. https://doi.org/10.1080/21642583.2025.2600780
8. Cao Y, Jacob J, Dharani S, Sivakumar M. Improved stability analysis for quaternion-valued neural networks with proportional and mixed time-varying delays. *Math Comput Simul.* 2025;242:270-278. https://doi.org/10.1016/j.matcom.2025.11.005
9. Sivaranjani K, Sivakumar M, Dharani S, Loganathan K, Ngmgyel N. Nonfragile synchronization of semi-Markovian jumping neural networks with time delays via sampled-data control and application to chaotic systems. *J Math.* 2021;2021(1):2562227. https://doi.org/10.1155/2021/2562227
10. Subramaniam S, Mani P. Adaptive synchronization of the switching stochastic neural networks with time-dependent delays. *Eur Phys J Spec Top.* 2025;234(8):1689-1699. https://doi.org/10.1140/epjs/s11734-024-01198-z
11. Viera-Martin E, Gómez-Aguilar JF, Solís-Pérez JE, Hernández-Pérez JA, Escobar-Jiménez RF. Artificial neural networks: a practical review of applications involving fractional calculus. *Eur Phys J Spec Top.* 2022;231(10):2059-2095. https://doi.org/10.1140/epjs/s11734-022-00455-3
12. Cohen MA, Grossberg S. Absolute stability of global pattern formation and parallel memory storage by competitive neural networks. *IEEE Trans Syst Man Cybern.* 1983;5:815-826. https://doi.org/10.1109/TSMC.1983.6313075
13. Liu Y, Wang Z, Huang X, Shen H. Finite-time multisynchronization of coupled discontinuous Cohen-Grossberg neural networks and its application in associative memory. *IEEE Trans Circuits Syst I Regul Pap.* 2025;72(11):7109-7119. https://doi.org/10.1109/TCSI.2025.3559485
14. Gospodinova E, Torlakov I. Information processing with stability point modeling in Cohen-Grossberg neural networks. *Axioms.* 2023;12(7):612. https://doi.org/10.3390/axioms12070612
15. Liu Y, Wang Z, Xiao M, Li Y, Shen H. μ-stability of multiple equilibria in Cohen-Grossberg neural networks and its application to associative memory. *Sci China Technol Sci.* 2023;66(9):2611-2624. https://doi.org/10.1007/s11431-022-2311-1
16. Boykov IV, Roudnev VA, Boykova AI. Stability of Cohen-Grossberg neural networks with time-dependent delays. *Tech Phys.* 2023;68(6):126-133. https://doi.org/10.1134/S1063784223040023
17. Ketencigil MM, Faydasicok O, Arik S. Novel criteria for robust stability of Cohen-Grossberg neural networks with multiple time delays. *Discrete Contin Dyn Syst Ser S.* 2022;15(11):3189. https://doi.org/10.3934/dcdss.2022081
18. Liu XZ, Wu KN, Ding X, Zhang W. Boundary stabilization of stochastic delayed Cohen-Grossberg neural networks with diffusion terms. *IEEE Trans Neural Netw Learn Syst.* 2021;33(8):3227-3237. https://doi.org/10.1109/TNNLS.2021.3051363
19. Kong F, Zhu Q, Karimi HR. Fixed-time periodic stabilization of discontinuous reaction-diffusion Cohen-Grossberg neural networks. *Neural Netw.* 2023;166:354-365. https://doi.org/10.1016/j.neunet.2023.07.017
20. Aouiti C, Bessifi M. Finite-time and fixed-time synchronization of fuzzy Clifford-valued Cohen-Grossberg neural networks with discontinuous activations and time-varying delays. *Int J Adapt Control Signal Process.* 2021;35(12):2499-2520. https://doi.org/10.1002/acs.3333
21. Huang J, Wu X, Tu Z. Exponential synchronization of Cohen-Grossberg neural networks with delays. *IEEE Access.* 2023;11:49992-49999. https://doi.org/10.1109/ACCESS.2023.3277986
22. Rakkiyappan R, Dharani S, Zhu Q. Synchronization of reaction-diffusion neural networks with time-varying delays via stochastic sampled-data controller. *Nonlinear Dyn.* 2015;79(1):485-500. https://doi.org/10.1007/s11071-014-1681-x

23. Jacob J, Dharani S. Finite-time synchronization of quaternion-valued neural networks with time-varying and proportional delay under hybrid sampled-data control with application to secure image encryption. *Complex Anal Oper Theory.* 2026;20(2):60. https://doi.org/10.1007/s11785-026-01913-9
24. Li R, Song Q, Liu Y. Projective synchronization of fractional-order quaternion-valued neural networks with time-varying delays and distributed delays on time scales. *Neurocomputing.* 2026;134719. https://doi.org/10.1016/j.neucom.2026.134719
25. Li TZ, Tan XW, Wang Y, Wang QK. Analysis of stability and quasi-synchronization in fractional-order neural networks with mixed delays, uncertainties, and external disturbances. *Fractal Fract.* 2026;10(1):73. https://doi.org/10.3390/fractalfract10010073
26. Du F, Lu JG. Novel methods of finite-time synchronization of fractional-order delayed memristor-based Cohen-Grossberg neural networks. *Nonlinear Dyn.* 2023;111(20):18985-19001. https://doi.org/10.1007/s11071-023-08880-2
27. Wu Z, Nie X. Finite-time synchronization of fractional-order quaternion-valued delayed Cohen-Grossberg neural networks. *Neural Process Lett.* 2023;55(9):12255-12271. https://doi.org/10.1007/s11063-023-11419-6
28. Zhou Z. Stability and synchronization of delayed fractional-order reaction-diffusion Cohen-Grossberg neural networks under perturbation and parameter mismatch. *Asian J Control.* 2026;28(3):1526-1543. https://doi.org/10.1002/asjc.3764
29. Yan H, Qiao Y, Duan L, Miao J. New results of quasi-projective synchronization for fractional-order complex-valued neural networks with leakage and discrete delays. *Chaos Solitons Fractals.* 2022;159:112121. https://doi.org/10.1016/j.chaos.2022.112121
30. Yang J, Li HL, Yang J, Zhang L, Jiang H. Quasi-synchronization and complete synchronization of fractional-order fuzzy BAM neural networks via nonlinear control. *Neural Process Lett.* 2022;54(4):3303-3319. https://doi.org/10.1007/s11063-022-10769-x
31. Wu A, Zhan N. Synchronization of uncertain chaotic neural networks via average-delay impulsive control. *Math Methods Appl Sci.* 2022;48(7):7213-7225. https://doi.org/10.1002/mma.8889
32. Babcock KL, Westervelt RM. Stability and dynamics of simple electronic neural networks with added inertia. *Phys D Nonlinear Phenom.* 1986;23(1-3):464-469. https://doi.org/10.1016/0167-2789(86)90152-1
33. Huang Q, Cao J, Liu Q. Synchronization of delayed inertial Cohen-Grossberg neural networks under adaptive feedback controller. *Int J Comput Intell Syst.* 2020;13(1):472-478. https://doi.org/10.2991/ijcis.d.200402.001
34. Xiong Y, Li Y, Lv H, *et al.* Fixed-time synchronization of Caputo/Conformable fractional-order inertial Cohen-Grossberg neural networks via event-triggered one/two-phase hybrid impulsive control. *Neural Process Lett.* 2025;57(1):7. https://doi.org/10.1007/s11063-024-11703-z
35. Kowsalya P, Mohanrasu SS, Kashkynbayev A, Gokul P, Rakkiyappan R. Fixed-time synchronization of inertial Cohen-Grossberg neural networks with state dependent delayed impulse control and its application to multi-image encryption. *Chaos Solitons Fractals.* 2024;181:114693. https://doi.org/10.1016/j.chaos.2024.114693
36. Sui X, Yang Y. Quasi-Mittag-Leffler projective synchronization of delayed chaotic fractional order neural network with mismatched parameters. *Fractal Fract.* 2025;9(6):379. https://doi.org/10.3390/fractalfract9060379
37. Zhang H, Chen X, Ye R, Stamova I, Cao J. Adaptive quasi-synchronization analysis for Caputo delayed Cohen-Grossberg neural networks. *Math Comput Simul.* 2023;212:49-65. https://doi.org/10.1016/j.matcom.2023.04.025
38. Zhang H, Yin X, Zhang H, Zhang W. New criteria on global Mittag-Leffler synchronization for Caputo-type delayed Cohen-Grossberg inertial neural networks. *AIMS Math.* 2023;8(12):29239-29259. https://doi.org/10.3934/math.20231497
39. Ding Z, Zhang H, Zeng Z, Yang L, Li S. Global dissipativity and quasi-Mittag-Leffler synchronization of fractional-order discontinuous complex-valued neural networks. *IEEE Trans Neural Netw Learn Syst.* 2021;34(8):4139-4152. https://doi.org/10.1109/TNNLS.2021.3119647
40. Podlubny I. *Fractional Differential Equations: An Introduction to Fractional Derivatives, Fractional Differential Equations, to Methods of Their Solution and Some of Their Applications.* Vol 198. San Diego, CA: Elsevier; 1998.
41. Duarte-Mermoud MA, Aguila-Camacho N, Gallegos JA, Castro-Linares R. Using general quadratic Lyapunov functions to prove Lyapunov uniform stability for fractional order systems. *Commun Nonlinear Sci Numer Simul.* 2015;22(1-3):650-659. https://doi.org/10.1016/j.cnsns.2014.10.008
42. Li HL, Hu C, Zhang L, Jiang H, Cao J. Complete and finite-time synchronization of fractional-order fuzzy neural networks via nonlinear feedback control. *Fuzzy Sets Syst.* 2022;443:50-69. https://doi.org/10.1016/j.fss.2021.11.004
43. Wang D, Zou J. Dissipativity and contractivity analysis for fractional functional differential equations and their numerical approximations. *SIAM J Numer Anal.* 2019;57(3):1445-1470. https://doi.org/10.1137/17M1121354
44. Zhang XL, Li HL, Yu Y, Zhang L, Jiang H. Quasi-projective and complete synchronization of

discrete-time fractional-order delayed neural networks. *Neural Netw.* 2023;164:497-507. https://doi.org/10.1016/j.neunet.2023.05.005

45. Huan M, Li C. Synchronization of inertial Cohen-Grossberg-type neural networks with reaction-diffusion terms. *Int J Control Autom Syst.* 2022;20(12):4059-4075. https://doi.org/10.1007/s12555-021-0721-9

Pavithra Ganeshan *received the B.Sc. and M.Sc. degrees in Mathematics from Government Arts College (Autonomous), Coimbatore, Tamil Nadu, India, in 2020 and 2023, respectively. She is currently pursuing the Ph.D. degree as a Research Scholar in the Department of Mathematics at Vellore Institute of Technology, Vellore, India. Her research interests include stability analysis, neural networks, fractional differential equations, and time-delay systems.*
https://orcid.org/0009-0006-6841-5087

Dharani Shanmugavel *received the B.Sc. degree in Mathematics from NGM College, Bharathiar University, Coimbatore, India, in 2010, the M.Sc. degree in Mathematics from Bharathiar University, Coimbatore, India, in 2012, the M.Phil. degree in Mathematics from Bharathiar University in 2013, and the Ph.D. degree in Mathematics from Bharathiar University, Coimbatore, India, in 2018. She was a Post doctoral Fellow in the Department of Mathematics, Gandhigram Rural Institute, Dindigul, India, under the DST-SERB National Post doctoral Fellowship Scheme from 2017 to 2018. She served as an Assistant Professor in the Department of Mathematics, Bannari Amman Institute of Technology, Erode, India, from 2018 to 2021. From 2021 to 2022, she worked as an Assistant Professor in the Department of Mathematics, School of Foundational Sciences, Kumaraguru College of Technology, Coimbatore, India. She is currently an Assistant Professor in the Department of Mathematics, School of Advanced Sciences, Vellore Institute of Technology, Vellore, India. She has published 41 research papers in reputed SCI journals. She also serves as a Reviewer for several SCI journals. Her current research interests include reaction-diffusion systems, stochastic stability, image encryption, nonlinear systems, fuzzy systems, time-delay systems, complex dynamical networks and chaotic systems.*
https://orcid.org/0000-0003-2557-5209

Sivakumar Muthusamy *received the B.Sc. degree in Mathematics from Kaamadhenu Arts and Science College, Sathyamangalam, Erode, India, in 2010, the M.Sc. degree in Mathematics from Sri Ramakrishna Mission Vidyalaya College of Arts and Science, Coimbatore, India, in 2012, the M.Phil. degree in Mathematics from Bharathiar University in 2013, and the Ph.D. degree in Mathematics from Bharathiar University, Coimbatore, India, in 2017. He is currently an Associate Professor in the Department of Mathematics, School of Advanced Sciences, Vellore Institute of Technology, Vellore, India. He also serves as a reviewer for several SCI journals. His current research interests include ordinary differential equations, partial differential equations and mathematical biology.*
https://orcid.org/0000-0003-3566-0239

This work is licensed under a Creative Commons Attribution 4.0 International License. The authors retain ownership of the copyright for their article, but they allow anyone to download, reuse, reprint, modify, distribute, and/or copy articles in IJOCTA, so long as the original authors and source are credited. To see the complete license contents, please visit http://creativecommons.org/licenses/by/4.0/.